Modal-Pushover-based Ground Motion Scaling Procedure for Nonlinear Analysis of Structures

by

Erol Kalkan[1] and Anil K. Chopra[2]

ABSTRACT

Earthquake engineering practice is increasingly using nonlinear response history analysis (RHA) to demonstrate performance of structures. This rigorous method of analysis requires selection and scaling of ground motions appropriate to design hazard levels. Presented herein is a modal-pushover-based scaling (MPS) method to scale ground motions for use in nonlinear RHA of buildings. In the MPS method, the ground motions are scaled to match (to a specified tolerance) a target value of the inelastic deformation of the first-mode inelastic SDF system whose properties are determined by first-mode pushover analysis. Appropriate for first-mode dominated structures, this approach is extended for structures with significant contributions of higher modes by considering elastic deformation of higher-mode SDF systems in selecting a subset of the scaled ground motions. Based on results presented for three actual buildings—4-story, 6-story, and 13-story—the accuracy and efficiency of the MPS procedure are established and its superiority over the ASCE-7 scaling procedure is demonstrated.

KEYWORDS: nonlinear analysis; seismic effects; drift; performance-based earthquake engineering.

1.0 INTRODUCTION

The maximum span of long-span bridges has been Seismic evaluation of existing structures and of proposed design of new structures is usually based on nonlinear static (or pushover) analysis procedures, but nonlinear response history analysis (RHA) is now being increasingly used. In the latter approach, the seismic demands are determined by nonlinear RHA of the structure for several ground motions. Procedures for selecting and scaling ground motion records for a site-specific hazard are described in building codes and have been the subject of much research in recent years.

Current performance-based design and evaluation methodologies prefer intensity-based methods to scale ground motions over spectral matching techniques that modify the frequency content and/or phasing of the record to match its response spectrum to the target spectrum. In contrast, intensity-based scaling methods preserve the original non-stationary content and only modify its amplitude. The primary objective of intensity-based scaling methods is to provide scale factors for a small number of ground motion records so that nonlinear RHA of the structure for these scaled records is accurate, i.e., it provides an accurate estimate in the median value of the engineering demand parameters (EDPs), and is efficient, i.e., it minimizes the record-to-record variations in the EDP. Scaling ground motions to match a target value of peak ground acceleration (PGA) is the earliest approach to the problem, which produces inaccurate estimates with large dispersion in EDP values for structures responding in nonlinear range [Nau and Hall 1984; Miranda 1993; Vidic et al. 1994; Shome and Cornell 1998]. Other scalar intensity measures (IMs) such as: effective peak acceleration, Arias intensity and effective peak velocity have also been found to be inaccurate and

[1] Senior Research Engineer, United States Geological Survey, Menlo Park, CA 94025, USA
[2] Professor, Dept. of Civil and Env. Engineering, University of California, Berkeley, CA 94720, USA

inefficient [Kurama and Farrow 2003]. None of the preceding IMs consider any property of the structure to be analyzed.

Including a vibration property of the structure led to improved methods to scale ground motions, e.g., scaling records to a target value of the elastic spectral acceleration, $A(T_1)$ from the code-based design spectrum or PSHA-based uniform hazard spectrum at the fundamental vibration period of the structure, T_1, provides improved results for structures whose response is dominated by their first-mode [Shome et al. 1998]. However, this scaling method becomes less accurate and less efficient for structures responding significantly in their higher vibration modes or far into the inelastic range [Mehanny 1999; Alavi and Krawinkler 2000; Kurama and Farrow 2003]. To consider higher mode response, a scalar IM that combines the spectral accelerations $A(T_1)$ and $A(T_2)$ at the first two periods and vector IM comprised of $A(T_1)$ and the ratio of $A(T_1)/A(T_2)$ have been developed [Bazzurro 1998; Shome and Cornell 1999]. Although this vector IM improves accuracy, it remains inefficient for near-fault records with a dominant velocity pulse [Baker and Cornell 2006].

To recognize the lengthening of the apparent period of vibration due to yielding of the structure, a scalar IM defined as a combination of $A(T_1)$ and $A(cT_1)$ where $c>1$, has been considered [Mehanny 1999; Cordova et al. 2000]; alternatively, scaling earthquake records to minimize the difference between its elastic response spectrum and the target spectrum has been proposed [Kennedy et al. 1984; Malhotra 2003; Alavi and Krawinkler 2004; Naeim et al. 2004; Youngs et al. 2007].

International Building Code (IBC) [ICBO 2006] and California Building Code (CBC) [ICBO 2007] require that earthquake records be scaled according to the ASCE-7 provisions [ASCE 2005]. For two dimensional analyses of regular structures, ground motions are scaled such that the average value of the 5%-damped elastic response spectra for a set of scaled motions is not less than the design response spectrum over the period range from $0.2T_1$ to $1.5T_1$. For structures having plan irregularities or structures without independent orthogonal lateral load resisting systems, where three-dimensional analyses need to be performed, ground motions should consist of appropriate horizontal components.

All the preceding scaling methods utilize IMs based on elastic response of the structure, but do not explicitly consider its inelastic response. They lead to scale factors that depend only on the structural period(s), independent of the structural strength. The elastic-response-based IMs may not be appropriate for near-fault sites where the inelastic spectral deformation can be significantly larger than corresponding elastic spectral deformation [Bozorgnia and Mahin 1998; Alavi and Krawinkler 2000; Baez and Miranda 2000; Chopra and Chintanapakdee 2004]. This limitation has been overcome in recently proposed IMs based on the inelastic deformation spectrum, leading to improved estimate of the median EDPs, and reduced dispersion of EDPs [Bazzurro and Luco 2004; Luco and Cornell 2007]. Based on incremental dynamic analyses response of generic frames to different intensity levels of near-fault ground motions demonstrated that scaling records with the IM defined as the inelastic deformation of the first-mode inelastic SDF system is accurate, efficient and sufficient compared to elastic-response-based IMs [Tothong and Luco 2007; Tothong and Cornell 2008]. Required in this approach are attenuation relationships for the inelastic deformation with given ground motion properties (magnitude, closest fault distance, site condition, etc.) and mean rate of occurrence of that hazard level [Tothong and Cornell 2008].

The objective of this paper is to develop a new method for selecting and scaling earthquake ground motion records in a form convenient for evaluating existing structures or proposed designs for new structures. The procedure presented explicitly considers structural strength and is based on the standard IM of spectral acceleration that is available from the USGS seismic hazard maps, where it is mapped for periods of 0.2 s and 1.0 s for the entire U.S. to facilitate construction of site-

specific design spectrum [Petersen et al. 2008], or it can be computed from the uniform hazard spectrum obtained by probabilistic seismic hazard analysis (PSHA) for the site.

Based on modal pushover analysis, the procedure presented herein explicitly considers the strength of the structure, obtained from the first-mode pushover curve and determines scaling factors for each record to match a target value of the deformation of the first-mode inelastic SDF system estimated by established procedures. Appropriate for first-mode dominated structures, this approach is extended for structures with significant contributions of higher modes. Based on results presented for three actual buildings—4-, 6-, and 13-story—the effectiveness of this scaling procedure is established and its superiority in terms of accuracy and efficiency over the ASCE-7 procedure is demonstrated.

2.0 MODAL-PUSHOVER-BASED SCALING

In the modal pushover-based scaling (MPS) procedure, each ground motion record is scaled by a scale factor selected to ensure that the peak deformation of the first-mode inelastic SDF system due to the scaled record is close enough to a target value of the inelastic deformation. The force-deformation relation for the first-mode inelastic SDF system is determined from the first-mode pushover curve. The target value of the inelastic deformation is the median deformation of the inelastic SDF system for a large ensemble of (unscaled) earthquake records compatible with the site-specific seismic hazard conditions. Nonlinear RHA of the inelastic SDF system provides the peak deformation of the system to each record in the ensemble, and the median of the data set provides the target value. Alternatively, the median deformation of the inelastic SDF system can be estimated as the deformation of the corresponding linearly elastic system, known directly from the target spectrum, multiplied by the inelastic deformation ratio; empirical equations for this ratio are available for systems with known yield-strength reduction factor [e.g., Ruiz-Garcia and Miranda 2002; Chopra and Chintanapakdee 2004].

For first-mode dominated structures, scaling earthquake records to the same target value of the inelastic deformation is expected be sufficient. Because higher vibration modes are known to contribute significantly to the seismic response of mid-rise and high-rise buildings, the MPS procedure checks for higher-mode compatibility of each record by comparing its scaled elastic spectral displacement response values at higher-mode vibration periods of the structure against the target spectrum. This approach ensures that each scaled earthquake record satisfies two requirements: (1) the peak deformation of the first-mode inelastic SDF system is close enough to the target value of the inelastic deformation; and (2) the peak deformation of the higher-mode (i.e., second-mode) elastic SDF system is not far from the target spectrum.

2.1 MPS Procedure: Summary

The MPS procedure is summarized below in a step-by-step form:

1. For the given site, define the target pseudo-acceleration response spectrum either as the PSHA-based uniform hazard spectrum, or code-based design spectrum, or the median pseudo-acceleration spectrum for a large ensemble of (unscaled) earthquake records compatible with the site-specific seismic hazard conditions.
2. Compute the frequencies ω_n (periods T_n) and $\boldsymbol{\phi}_n$ of the first few modes of elastic vibration of the structure.

First-mode Dominated Structures

3. Develop the base shear-roof displacement V_{b1}-u_{r1} relation or pushover curve by nonlinear static analysis of the structure subjected to gradually increasing lateral forces with an invariant force distribution $\mathbf{s}_1^* = \mathbf{m}\boldsymbol{\phi}_1$, associated with the first-mode, where $\mathbf{m}$ is the structural mass matrix. Gravity loads, including those present on the interior (gravity) frames, are applied before starting the pushover analysis.

4. Idealize the pushover curve and select a hysteretic model for cyclic deformations, both appropriate for the structural system and materials [Han and Chopra 2005; Bobadilla and Chopra 2007]. Determine the yield-strength reduction factor R_y (equals strength required for the structure to remain elastic divided by the yield strength of the structure) from: $R_y = M_1^* \bar{A}_1 / V_{b1y}$, where M_1^* is the effective modal mass and V_{b1y} is the yield point value of base shear determined from the idealized pushover curve.

5. Convert the idealized pushover curve to the force-deformation $F_{s1}/L_1 - D_1$ relation of the first-mode inelastic SDF system by utilizing $F_{s1}/L_1 = V_{b1}/M_1^*$ and $D_1 = u_{r1}/\Gamma_1\phi_{r1}$ in which $L_1 = \phi_1 \mathbf{m} \boldsymbol{\iota}$, ϕ_{r1} is the value of $\boldsymbol{\phi}_1$ at the roof, $\Gamma_1 = (\phi_1^T \mathbf{m} \boldsymbol{\iota})/(\phi_1^T \mathbf{m} \phi_1)$ and each element of the influence vector $\boldsymbol{\iota}$ is equal to unity.

6. For the first-mode inelastic SDF system, establish the target value of deformation $\bar{D}_1^I$ from $\bar{D}_1^I = C_R \bar{D}_1$, where $\bar{D}_1 = (T_1/2\pi)^2 \bar{A}_1$ and $\bar{A}_1$ is the target pseudo-spectral acceleration at period T_1, and C_R is determined from an empirical equation (shown in the next section) for the inelastic deformation ratio corresponding to the yield-strength reduction factor R_y, determined in Step 4.

7. Compute the peak deformation $D_1^I = \max|D_1(t)|$ of the first-mode inelastic SDF system defined by the force deformation relation developed in Steps 4 and 5, and damping ratio ζ_1. The initial elastic vibration period of the system is $T_1 = 2\pi (L_1 D_{1y}/F_{s1y})^{1/2}$. For a SDF system with known T_1 and ζ_1, D_1^I can be computed by nonlinear RHA due to one of the selected ground motions $\ddot{u}_g(t)$ multiplied by a scale factor SF, to be determined to satisfy Step 8, by solving

$$\ddot{D}_1 + 2\zeta_1\omega_1\dot{D}_1 + F_{s1}\left[D_1, \dot{D}_1\right]/L_1 = -(SF)\ddot{u}_g(t) \quad (1)$$

8. Compare the normalized difference between the target value of the deformation $\bar{D}_1^I$ of the first-mode inelastic SDF system (Step 6) and the peak deformation D_1^I, determined in Step 7 against a specified tolerance, ε

$$\Delta_1 = \left|\bar{D}_1^I - D_1^I\right|/\bar{D}_1^I < \varepsilon \quad (2)$$

9. Determine the scale factor *SF* such that the scaled record $(SF)\ddot{u}_g(t)$ satisfies the criterion of Eq. (2). Because Eq. (1) is nonlinear, *SF* cannot be determined *a priori*, but requires an iterative procedure starting with an initial guess. Starting with *SF* = 1, Steps 7 and 8 are implemented and repeated with modified values of *SF* until Eq. (2) is satisfied. Successive values of *SF* are chosen by trial and error or by a convergence algorithm, e.g., Newton-Raphson iteration procedure. For a given ground motion, if the Eq. 2 is satisfied by more than one SF, the SF closest to one should be preferred.

Repeat Steps 7 and 8 for as many records as deemed necessary; obviously the scaling factor *SF* will be different for each record. These scaling factors will be shown to be appropriate for structures that respond dominantly in the first-mode.

Higher-mode Considerations

10. Establish target values of deformation of higher-mode SDF systems, treated as elastic systems, from the target spectrum $\bar{D}_n = (T_n/2\pi)^2 \bar{A}_n$, where the mode number *n* = 2. We have found that the second-mode is mostly adequate for buildings susceptible to higher-mode effects.

11. By linear RHA, calculate the peak deformation $D_2 \equiv \max_t |D_2(t)|$ of the *n*th-mode elastic SDF system with known T_2 and ζ_2 due to a selected ground motion $\ddot{u}_g(t)$ multiplied by its scale factor *SF* determined in Step 9.

12. Compute the normalized difference between the target value of deformation $\bar{D}_2$ (Step 10) and the peak deformation determined in Step 11.

$$\Delta_2 = \left|\bar{D}_2 - D_2\right| / \bar{D}_2 \qquad (3)$$

and rank the scaled records based on their Δ_2 value; the record with the lowest average Δ_2 is ranked the highest.

13. From the ranked list, select the final set of records with their scale factors determined in Step 9 to be used in nonlinear RHA of the structure.

3.0 ESTIMATING SDF-SYSTEM INELASTIC DEFORMATION

The inelastic deformation ratio C_R is required in Step 6 to estimate the deformation of the inelastic SDF system. Such equations were first developed by Veletsos and Newmark [1960] as a function of elastic vibration T_n and ductility factor μ. However, in selecting and scaling ground motion records for nonlinear RHA of an existing building or of a proposed design of a new building, the inelastic deformation ratio should be expressed as a function of T_n and the yield-strength reduction factor R_y; these quantities are determined in Steps 7 and 4, respectively. The inelastic deformation ratio can be expressed as a function of elastic vibration period and yield-strength reduction factor R_y. Response data for 216 ground motions recorded on NEHRP site classes B, C, and D demonstrated that the mean inelastic deformation ratio is influenced little by soil condition, by magnitude if R_y < 4 (but significantly for larger R_y), or by site-to-fault distance so long as it exceeds 10 km [Ruiz-Garcia and Miranda 2002]. Regression analysis of these data led to an equation for the inelastic deformation ratio as a function of T_n and R_y; this equation is restricted to elastoplastic systems.

Median values of C_R have been presented for non-degrading bilinear hysteretic systems subjected to seven ensembles of far-fault ground motions (each with 20 records), representing large or small earthquake magnitude and distance, and NEHRP site classes, B, C, or D; and for two ensembles of near-fault ground motions. Regression analysis of these data led to the empirical C_R equation [Chopra and Chintanapakdee 2004]:

$$C_R = 1 + \left[(L_R - 1)^{-1} + \left(\frac{a}{R_y^b} + c \right) \left(\frac{T_1}{T_c} \right)^d \right]^{-1} \qquad (4)$$

in which, the limiting value of C_R at $T_n = 0$ is:

$$L_R = \frac{1}{R_y} \left(1 + \frac{R_y - 1}{\alpha} \right) \qquad (5)$$

where α is the post-yield stiffness ratio and T_c is the period separating the acceleration and velocity-sensitive regions of the target spectrum; the parameters in Eq. (4) are: a=61, b=2.4, c=1.5, and d=2.4.

Equations (4) and (5) and values of their parameters are valid for far-fault ground motions, independent of (1) earthquake magnitude and distance; and (2) NEHRP site class B, C, and D; and also for near-fault ground motions.

4.0 CODE-BASED SCALING PROCEDURE

The procedures and criteria in the 2006 IBC and 2007 CBC for the selection and scaling of ground motions for use in nonlinear RHA of structures are based on the ASCE-7 provisions [ASCE 2005]. According to ASCE-7, earthquake records should be selected from events of magnitudes, fault distance and source mechanisms that comply with the maximum considered earthquake. If the required number of appropriate records is not

available, appropriate simulated ground motions may be included to make up the total number required.

For two-dimensional analysis of symmetric-plan buildings, ASCE-7 requires intensity-based scaling of ground motion records using appropriate scale factors so that the average value of the 5%-damped response spectra for the set of scaled records is not less than the design response spectrum over the period range from $0.2T_1$ to $1.5T_1$. The design value of an EDP—member forces, member deformations or story drifts—is taken as the average value of the EDP over seven (or more) ground motions, or its maximum value over all ground motions, if the system is analyzed for fewer than seven ground motions.
The ASCE-7 scaling procedure does not insure a unique scaling factor for each record; obviously, various combinations of scaling factors can be defined to insure that the average spectrum of scaled records remains above the design spectrum (or amplified spectrum incase of 3-D analyses) over the specified period range. Because it is desirable to scale each record by the smallest possible factor, an algorithm is developed and used in applying the code-scaling procedure in the evaluation section. This algorithm is provided at Kalkan and Chopra (2008).

5.0 GROUND MOTIONS & SYSTEMS ANALYZED

A total of twenty one near-fault strong earthquake ground motions were compiled from the Next Generation of Attenuation project earthquake ground motion database [Power et al. 2006]. These motions were recorded during seismic events with moment magnitude, M $\geq$ 6.5 at closest fault distances, $R_{cl} \leq 12$ km and belonging to NEHRP site classification C and D. The selected ground motion records and their characteristic parameters are listed in Table 1. Shown in Fig. 1a are the pseudo-acceleration response spectrum for each ground motion and the median of the 21 response spectra. The median spectrum is taken to be the design spectrum for purposes of evaluating the MPS and ASCE-7 scaling procedures. The median spectrum of the ground motion ensemble is presented next in Fig. 1b as a four-way logarithmic plot, together with its idealized version (dashed-line). The idealized spectrum is divided logically into three period ranges: the long-period region to the right of point d, $T_n > T_d$, is called the displacement-sensitive region; the short-period region to the left of point c, $T_n < T_c$, is called the acceleration-sensitive region; and the intermediate-period region between points c and d, $T_c < T_n < T_d$, is called the velocity-sensitive region [Chopra 2007; Section 6.8]. Note that the velocity-sensitive region is unusually narrow, which is typical of near-fault ground motions.

The buildings selected to evaluate the efficiency and accuracy of the MPS method are existing four-, six-, and thirteen-story steel special moment resisting frame (SMRF) buildings representative of low-rise and mid-rise building-types in California. The six and thirteen-story buildings are instrumented, and their motions have been recorded during past earthquakes. The first three natural vibration periods and modes of each building are shown in Fig. 2 and the first-mode pushover curves in Fig. 3, where P-Δ effects are included. A description of these buildings and complete details of their analytical models are reported at Kalkan and Chopra (2008).

6.0 EVALUATION OF MPS PROCEDURE

The efficiency and accuracy of the MPS and ASCE-7 scaling procedures will be evaluated. A scaling procedure is considered efficient if the dispersion of EDPs due to the scaled records are small; it is accurate if the median value of the EDPs due to scaled ground motions is close to the benchmark results, defined as the median values of EDPs, determined by nonlinear RHA of the building to each of the 21 unscaled ground motions. In this section, the median values of EDPs determined from a set of 7 ground motions, scaled according to MPS and ASCE-7 scaling procedures, will be compared. The median value $\hat{x}$, defined as the geometric mean, and the dispersion measure, δ of n observed values of x_i are calculated from

$$\hat{x} = \exp\left[\frac{\sum_{i=1}^{n} \ln x_i}{n}\right] \qquad \delta = \left[\frac{\sum_{i=1}^{n} (\ln x_i - \ln \hat{x})^2}{n-1}\right]^{1/2} \tag{4}$$

The EDPs selected are peak values of story drift ratio, i.e., peak relative displacement between two consecutive floors normalized by story height; floor displacements normalized by building height; column and beam plastic rotations. Fig. 4 shows the benchmark EDPs for all three buildings; results from individual records are also included to demonstrate the large dispersion. Almost all of the excitations drive all three buildings well into the inelastic range as shown in Fig. 3 where the roof displacement values due to 21 ground motions are identified on the first-mode pushover curve. Also shown is the median value.

6.1 Evaluation of MPS Concept

As a first step in evaluating the concept underlying the MPS procedure, the target value of deformation $\bar{D}_1^I$ is computed not as described in Step 6 of the procedure, but as the median value of peak deformation of the first-mode inelastic SDF system due to 21 ground motions determined by nonlinear RHA. The MPS method utilizing this $\bar{D}_1^I$ value is denoted henceforth as MPS*. The 21 ground motions are divided into 3 sets each containing 7 records (Table 1). The records in each set are selected randomly from at least 3 different earthquakes to avoid any dominant influence of a single event on the ground motion set. An appropriate scale factor for each record is determined by implementing Steps 1-8 of the MPS procedure.

Efficiency and accuracy of the MPS* procedure are evaluated for each ground motion set, separately by comparing the median values of EDPs determined by nonlinear RHA of the building due to the 7 scaled records against the benchmark EDPs. Representative comparisons are depicted in Fig. 5 for the three buildings considering Ground Motion Set 1. Included are the EDPs due to each of the 7 scaled ground motions to show the dispersion of the data. Ground Motion Set 2 and 3 yield identical results [Kalkan and Chopra 2008].

These results identifies that the median values of EDPs due to every small (7) subset of scaled ground motion closely match the benchmark results, which were determined from a large (21) set of ground motions. The dispersion of the EDP values due to the 7 scaled records about their median value is much smaller compared to the data for the 21 unscaled records in Fig. 4. These results collectively demonstrate that the concept underlying the MPS procedure is accurate and efficient in scaling records for nonlinear RHA of buildings.

6.2 Evaluation of MPS and Code-Based Scaling Procedures

The preceding implementation of the MPS concept is the same as the MPS procedure described earlier, except for how $\bar{D}_1^I$ was computed. Previously, the exact value of $\bar{D}_1^I$ was determined by nonlinear RHA of the first-mode inelastic SDF system, but it will now be estimated according to Step 6, using an empirical equation for C_R, in accordance with the MPS procedure. In utilizing C_R equation, zero post-yield stiffness is assumed, although the idealized first-"mode" SDF systems have negative post-yield stiffness. This choice is dictated by the fact that the original C_R equation was determined for stable systems with non-negative post-yield stiffness ratio [Chopra and Chintanapakdee 2004]. In C_R equation, using zero post-yield stiffness seems to be plausible, because the variability in the peak displacement demand is not affected significantly by the hysteretic behavior (Kurama and Farrow, 2003; Gupta and Kunnath, 1998). Fig. 6 compares the "exact" target value of deformation $\bar{D}_1^I$ (continuous horizontal line) with estimated target value of deformation $\bar{D}_1^I$ (dashed horizontal line) using the C_R equation with zero post-yield stiffness; D_1^I values from individual records for each of the three buildings are also included. The difference between the "exact" and estimated values of $\bar{D}_1^I$ is 4, 9, and 12% of "exact" $\bar{D}_1^I$ values for the 4-, 6-, and 13-story buildings, respectively.

An appropriate scale factor for each record is then determined in accordance with two procedures: Steps 1-8 of the MPS procedure and the ASCE–7 procedure. The EDPs determined by nonlinear RHA of the structure due to a set of 7 ground motions scaled according to MPS and ASCE-7 procedures are compared against the benchmark EDPs. Figs. 6-8 present such comparisons for the three buildings considering Set 1 ground motions. The other two sets provide visually identical results [Kalkan and Chopra 2008].

These results demonstrate that the MPS procedure is much superior compared to the ASCE-7 procedure for scaling ground motion records. This superiority is apparent in two respects: First, for each building and each ground motion set, the ground motions scaled according to the MPS procedure lead to median values of EDPs that are much closer to the benchmark values than the corresponding results based on the ASCE-7 procedure. Second, the dispersion in the EDP values due to the 7 scaled records around the median value is much smaller when the records are scaled according to the MPS procedure compared to the ASCE-7 scaling procedure. However, even with MPS scaling, the dispersion of EDPs for the upper stories of 6- and 13-story buildings is noticeable (particularly for Ground Motion Set 2 as shown later), indicating that the higher-mode contributions to the seismic demands are significant. These factors will be considered later in Steps 10-13 of the MPS procedure.

An alternative way of comparing MPS and ASCE-7 scaling methods is based on the ratio of the EDP value due to a scaled record and the benchmark value. The deviation of the median Δ of this ratio from unity is an indication of the error or bias in estimating the median EDP value, and the dispersion σ of this ratio is an indication of the scatter in the individual EDPs, determined from the scaled ground motions. Included also in the comparison is the MPS* procedure based on "exact" values of $\bar{D}_1^I$ instead of Step 6.

Fig. 9 presents the median Δ of the EDP ratio for story drifts determined from records scaled according to the MPS*, MPS, and ASCE-7 scaling methods. Comparing these Δ values against 1.0, it is apparent that the MPS* method is most accurate (least biased), the MPS method is only slightly less accurate. The bias in the MPS methods is generally less than 20%. The ASCE-7 method is least accurate generally overestimates the EDPs, with the overestimation exceeding 50% in some cases.

Fig. 10 presents the dispersion of the EDP ratio for story drifts determined from records scaled according to the MPS*, MPS, and ASCE-7 scaling methods. It is apparent that the MPS* scaling method leads to the smallest dispersion, and it becomes only slightly larger in the MPS method. Dispersion is largest in the ASCE-7 scaling method, becoming unacceptably large for some combinations of buildings and ground motion sets.

7.0 MULTI-MODE CONSIDERATIONS

As demonstrated in preceding section, the MPS method based solely on the first-mode inelastic SDF system (steps 1-9 of the method) is superior over the ASCE-7 scaling method. Considering the higher modes of vibration is expected to improve the method further for mid-rise and high-rise buildings [Tothong and Cornell, 2008; Tothong and Luco, 2007; Luco and Cornell 2007].

The 21 records scaled based on the first-mode response only (steps 1-9 of the method) are ranked by accounting for higher mode response according to steps 10-13 of the method. Only one higher mode, the second mode, was considered for the 6 and 13-story buildings. The seven records with the highest ranks (see step-12) were defined as Ground Motion Set 4. Note that this set is different for each building.

Considering higher modes in selecting ground motions in the MPS method provides accurate estimates of the median EDPs and reduces the record-to-record variability (compared to the results achieved by Ground Motion Sets 1-3). This improved accuracy and efficiency is demonstrated in Figure 11, where the Δ and σ—the median value of the ratio of the estimated story drift to its benchmark value, and dispersion of this ratio—are

plotted for the four set of ground motions. It is apparent that Ground Motion Set 4 is more accurate and efficient than Ground Motion Sets 1 though 3.

The improvement achieved for these buildings is modest because the higher-mode computations are not especially significant in the response of selected buildings. Such improvement is expected to be more pronounced in the case of taller buildings responding significantly in their higher modes.

8.0 CONCLUSIONS

A modal-pushover-based scaling (MPS) method has been developed to scale ground motions for use in nonlinear response history analysis (RHA) of buildings. In the MPS method, the ground motions are scaled to match (to a specified tolerance) a target value of the inelastic deformation of the first-mode inelastic SDF system—its properties determined by first-mode pushover analysis—and the elastic deformation of higher-mode SDF systems are considered in selecting a subset of the scaled ground motions.

The median values of engineering demand parameters (EDPs)—floor displacement, story drifts, and plastic rotations—due to three sets of 7 ground motions scaled by two methods—MPS and ASCE-7—were computed by nonlinear RHA of the building and compared against the benchmark values of EDPs, determined by nonlinear RHA of the building for 21 unscaled records. Presented for 4-, 6-, and 13-story existing steel–SMRF buildings, such comparison led to the following conclusions:

1. Even for the most intense near-fault ground motions, which represent a severe test, the MPS method estimates the median value of seismic demands to a good degree of accuracy (within 20%t of the benchmark value). In contrast, the ASCE-7 scaling method overestimates the demand by 20 to 50% for 4-, and 6-story building, and its overestimation exceeds 50% for 13-story building. The dispersion of responses due to ground motion scaled by the MPS method is much smaller compared to the ASCE-7 scaling method; in the latter method, dispersion is unacceptably large for some combinations of buildings and ground motions sets. Thus, the MPS method is much more accurate, as well as efficient (as defined earlier) compared to the ASCE-7 scaling method.
2. Using the exact value of target deformation (as in MPS*), defined as the median deformation of the first-mode inelastic SDF system for a large ensemble of unscaled records determined by nonlinear RHA, leads to the most accurate and efficient version of the MPS method. Because this rigorous approach is not suitable for practical application, the target deformation may be estimated from the deformation of the corresponding linear system, available from the design spectrum, and empirical equations for the inelastic deformation ratio. The increase in bias and dispersion resulting from this approximation is small. The resulting practical version of the MPS method uses attenuation relations for elastic spectral ordinates that are currently available; new attenuation relations for inelastic spectral deformation are not required.
3. For first-mode dominated structures, scaling earthquake records to the target value of the inelastic deformation is sufficient in producing accurate estimates of median EDPs and in reducing the dispersion of EDPs due to individual ground motions. For mid-rise and high-rise buildings where higher vibration modes are known to contribute significantly to the seismic response, the MPS method requires an additional step to rank the scaled ground motions based on the closeness of the elastic deformation of higher-mode elastic SDF systems to their target values. Selecting a subset of highest-ranked ground motions leads to a method that is more accurate and efficient for estimating seismic demands for taller buildings.

This study has focused on developing the MPS method for scaling ground motions and its initial evaluation, which has been limited to low- and mid-rise steel SMRFs; stable force deformation

relations were considered and P-Δ effects were excluded.

9.0 ACKNOWLEDGMENT

Dr. Kalkan wishes to acknowledge the generous support of the Earthquake Engineering Research Institute for providing him the 2008 EERI/FEMA NEHRP Professional Fellowship in Earthquake Hazard Reduction for the research study "Preparation of practical guidelines to select and scale earthquake records for nonlinear response history analysis of structures".

10.0 REFERENCES

Alavi, B., and Krawinkler, H. (2000). "Consideration of near-fault ground motion effects in seismic design," Proc. of the 12th World Conference on Earthquake Engineering, Paper No. 2665, Auckland, New Zealand.

Alavi, B., and Krawinkler, H. (2004). "Behavior of moment-resisting frame structures subjected to near-fault ground motions," Eq. Eng. and Str. Dyn., Vol. 33, No. 6, pp. 687-706.

American Society of Civil Engineers (2005), ASCE-7 Minimum Design Loads for Buildings, Reston, VA.

Anderson, J., and Bertero, V. V. (1991). "Seismic performance of an instrumented six-story steel building," Earthquake Engineering Research Center, University of California, Berkeley, Report No. 1991-11, 134 p.

Báez, J. I., and Miranda, E. (2000). "Amplification factors to estimate inelastic displacement demands for the design of structures in the near field," Proc. of the Twelfth World Conf. on Eq. Eng., Paper No. 1561, Auckland, New Zealand.

Baker, J. W., and Cornell, A. C. (2006). "Spectral shape, epsilon and record selection," Earthquake Engineering & Structural Dynamics, Vol. 35, No. 9, pp. 1077-1095.

Bazzurro, P., 1998. Probabilistic Seismic Demand Analysis, Ph.D. thesis, Dept. of Civil and Env. Eng., Stanford University, CA. (Available online at http://www.stanford.edu/group/rms/Thesis/index.html; last accessed on 06/2008).

Bazzurro, P., and Luco, N. (2004). "Parameterization of Non-Stationary Acceleration Time Histories. Lifelines Program Project 1G00 Addenda. Pacific Earthquake Engineering Research (PEER) Center, University of California: Berkeley, CA, 83 p.

Bazzurro, P., and Luco, N. (2006). "Do scaled and spectrum-matched near-source records produce biased nonlinear structural responses," Proc. of the 8th National Conf. on Eq. Eng., Paper No. 1029, San Francisco, CA.

Bozorgnia, Y., and Mahin, S. A. (1998). "Ductility and strength demands of near-fault ground structure-specific scalar intensity measures 389 motions of the Northridge earthquake," Proceedings of the 6th U.S. National Conf. on Eq. Eng., Seattle, WA.

Chopra, A.K. (2001). Dynamics of Structures: Theory and Applications to Eq. Eng., 2nd Ed., Prentice Hall, Englewood Cliffs, N.J.

Chopra, A. K., and Chinatanapakdee, C. (2004). "Inelastic Deformation Ratios for Design and Evaluation of Structures: Single-Degree-of-Freedom Bilinear Systems," J. of Str. Eng. (ASCE), Vol. 130, No. 9, pp. 1304-1319.

Cordova, P. P., Deierlein, G. G., Mehanny, S. S. F., and Cornell, C. A., 2000. Development of a two-parameter seismic intensity measure and probabilistic assessment procedure, Proceedings of the 2nd U.S.-Japan Workshop on Performance-Based Seismic Design Methodology for Reinforced Concrete Building Structures, PEER Report 2000/10, Pacific Earthquake Engineering Research Center, University of California, Berkeley, CA.

International Conference of Building Officials (2006). International Building Code, Whittier, CA.

International Conference of Building Officials (2007). California Building Code, Whittier, CA.

Kalkan, E., and Chopra, A. K. (2008). "Modal-Pushover-based Ground Motion Scaling Procedure," Eq. Eng. Res. Center. Report, University of California Berkeley, CA, p. 49.

Krawinkler, H., and Al-Ali, A. (1996). "Seismic demand evaluation for a 4-story steel frame structure damaged in the Northridge earthquake," The Structural Design of Tall Buildings, Vol. 5, No. 1, pp. 1-27.

Kennedy, R. P., Short, S. A., Merz, K. L., Tokarz, F. J., Idriss, I. M., Power, M. S., and Sadigh, K. (1984). "Engineering characterization of ground motion-task 1: Effects of characteristics of free-field motion on structural response," NUREG/CR-3805, U.S. Regulatory Commission, Washington, D.C.

Kurama, Y., and Farrow, K. (2003). "Ground motion scaling methods for different site conditions and structure characteristics," Eq. Eng. and Str. Dyn., Vol. 32, No. 15, pp. 2425-2450.

Lilhhand, K., and Tseng, W. S. (1989). "Development and application of realistic earthquake time histories compatible with multiple damping design spectra," Proc. of the 9th World Conf. on Eq. Eng. Tokyo-Kyoto, Japan, Vol. 2, pp. 819-830.

Luco, N., and Cornell, A. C. (2007). "Structure-Specific Scalar Intensity Measures for Near-Source and Ordinary Earthquake Ground Motions," Earthquake Spectra, Vol. 23, No. 2, pp. 357–392.

Malhotra, P. K. (2003). "Strong-Motion Records for Site-Specific Analysis," Earthquake Spectra, Vol. 19, No. 3, pp. 557-578.

Mehanny, S. S. F. (1999). "Modeling and Assessment of Seismic Performance of Composite Frames with Reinforced Concrete Columns and Steel Beams," Ph.D. thesis, Dept. of Civil and Env. Eng., Stanford University, California.

Miranda, E. (1993). "Evaluation of site-dependent inelastic seismic design spectra," J. of Str. Eng. (ASCE), Vol. 119, No. 5, pp. 1319–1338.

Naeim, F., Alimoradi, A., and Pezeshk, S. (2004). "Selection and scaling of ground motion time histories for structural design using genetic algorithms," Earthquake Spectra, Vol. 20, No. 2, pp. 413-426.

Nau, J., and Hall, W. (1984). "Scaling methods for earthquake response spectra," J. of Str. Eng. (ASCE), Vol. 110, No. 91-109.

OpenSEES. Open Source finite element platform for earthquake engineering simulations 2006. University of California Berkeley, Pacific Earthquake Engineering Center. (Available online at http://opensees.berkeley.edu/; last accessed on 06/2008).

Petersen, M. D., Frankel, A. D., Harmsen, S. C., Mueller, C. S., Haller, K. M., Wheeler, R. L., Wesson, R. L., Zeng, Y., Boyd, O. S., Perkins, D. M., Luco, N., Field, E. H., Wills, C. J., and Rukstales, K. S., (2008). "Documentation for the 2008 Update of the United States National Seismic Hazard Maps," U.S. Geological Survey Open-File Report 2008–1128, 61 p. (Available online at: http://pubs.usgs.gov/of/2008/1128/; last accessed on 06/2008).

Power, M., Chiou, B., Abrahamson, N., and Roblee, C. 2006. "The Next Generation of Ground Motion Attenuation Models" (NGA) project: An overview," In Proc. of the Eighth National Conf. on Eq. Eng., Paper No. 2022, San Francisco, CA.

Ruiz-Garcia, J., and Miranda, E. (2002). "Inelastic displacement ratios for evaluation of existing structures," Eq. Eng. and Str. Dyn., Vol. 31, No. 3. pp. 539-560.

Shome, N., and Cornell, A. C. (1998). "Normalization and scaling accelerograms for nonlinear structural analysis," Prof. of the 6th U.S. National Conf. on Earthquake Engineering, Seattle, WA.

Shome, N., Cornell, C. A., Bazzurro, P., and Carballo, J. E., 1998. Earthquakes, records, and nonlinear responses, Earthquake Spectra, Vol. 14, No.3, pp. 469–500.

Shome, N., and Cornell, C. A., 1999. Probabilistic Seismic Demand Analysis of Nonlinear Structures, Reliability of Marine Structures Program Report No. RMS-35, Dept. of Civil and Env. Eng., Stanford University, CA. (Available online at http://www.stanford.edu/group/rms/Thesis/index.html; last accessed on 06/2008).

Tothong, P., and Cornell, A. C. (2008). "Structural performance assessment under near-source pulse-

like ground motions using advanced ground motion intensity measures," Eq. Eng. and Str. Dyn. Vol. 37, No. 7, pp. 1013-1037.

Veletsos, A. S., and Newmark, N. M. (1960). "Effect of inelastic behavior on the response of simple systems to earthquake motions," Proc. of the Second World Conf. on Eq. Eng., Tokyo, Japan, Vol. II, pp. 895–912.

Vidic, T. Fajfar, P., and Fischinger, M. (1994). "Consistent inelastic design spectra: Strength and displacement," Eq. Eng. and Str. Dyn., Vol. 23, No. 5, pp. 507-521.

Youngs, R. Power, M., Wang, G., Makdisi, F., and Chin, C. C. (2007). "Design Ground Motion Library (DGML) – Tool for Selecting Time History Records for Specific Engineering Applications (Abstract)," SMIP07 Seminar on Utilization of Strong-Motion Data, pp. 109 – 110. (Available online at http://www.conservation.ca.gov/cgs/smip/docs/seminar /SMIP07/Pages/Paper8_Youngs.aspx; last accessed on 06/2008).

Table 1: Selected Earthquake Ground Motions

No.	Earthquake	Year	Station	M	R_{cl} (km)	V_{S30} (m/s)	PGA (g)	PGV (cm/s)	PGD (cm)	Ground Motion Set No.
1	Tabas, Iran	1978	Tabas	7.4	2.1	767	0.85	110.3	61.1	2
2	Imperial Valley	1979	EC Meloland Overpass FF	6.5	0.1	186	0.31	79.3	28.1	2
3	Imperial Valley	1979	El Centro Array #7	6.5	0.6	211	0.42	80.2	41.0	3
4	Superstition Hills	1987	Parachute Test Site	6.5	1.0	349	0.46	74.8	36.3	1
5	Loma Prieta	1989	LGPC	6.9	3.9	478	0.78	77.2	42.7	3
6	Erzincan, Turkey	1992	Erzincan	6.7	4.4	275	0.49	72.9	24.8	2
7	Northridge	1994	Jensen Filter Plant	6.7	5.4	373	0.75	77.8	31.9	1
8	Northridge	1994	Newhall - W Pico Canyon Rd	6.7	5.5	286	0.39	76.6	43.1	3
9	Northridge	1994	Rinaldi Receiving Sta	6.7	6.5	282	0.63	109.2	28.3	3
10	Northridge	1994	Sylmar - Converter Sta	6.7	5.4	251	0.75	109.4	45.8	2
11	Northridge	1994	Sylmar - Converter Sta East	6.7	5.2	371	0.68	87.3	31.7	1
12	Northridge	1994	Sylmar - Olive View Med FF	6.7	5.3	441	0.71	97.4	22.4	3
13	Kobe, Japan	1995	Port Island	6.9	3.3	198	0.26	62.3	29.6	2
14	Kobe, Japan	1995	Takatori	6.9	1.5	256	0.65	118.8	33.4	1
15	Kocaeli, Turkey	1999	Yarimca	7.4	4.8	297	0.31	60.5	54.7	1
16	Chi-Chi, Taiwan	1999	TCU052	7.6	0.7	579	0.35	131.9	183.2	2
17	Chi-Chi, Taiwan	1999	TCU065	7.6	0.6	306	0.68	99.5	81.8	1
18	Chi-Chi, Taiwan	1999	TCU068	7.6	0.3	487	0.54	206.1	336.3	3
19	Chi-Chi, Taiwan	1999	TCU084	7.6	11.2	553	0.79	92.7	28.8	2
20	Chi-Chi, Taiwan	1999	TCU102	7.6	1.5	714	0.24	93.9	65.7	1
21	Duzce, Turkey	1999	Duzce	7.2	6.6	276	0.42	71.0	46.3	3

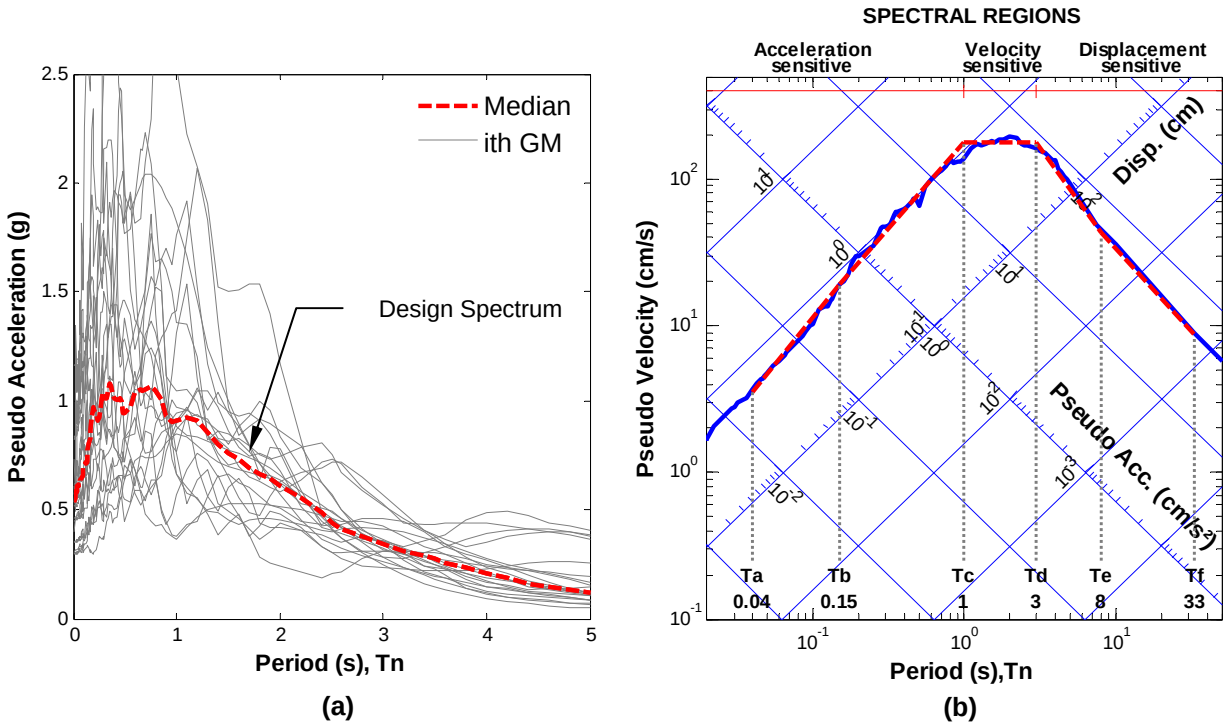

Figure 1: (a) Median elastic response spectrum for the selected ensemble of ground motions shown by a solid line, together with its idealized version in dashed line; spectral regions are

identified; (b) Individual response spectra for 21 ground motions and their median response spectrum; ζ= 5%.

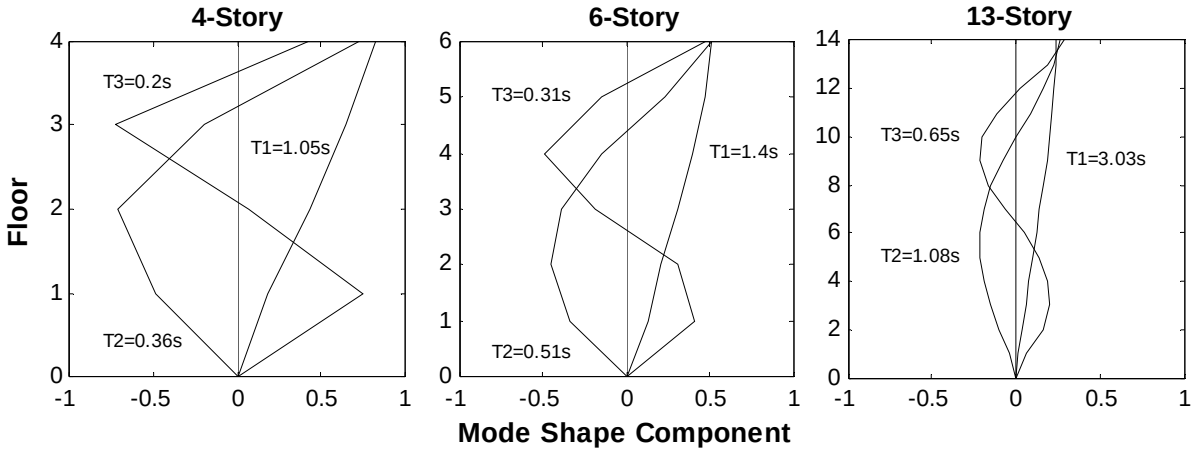

Figure 2: Natural vibration periods and modes of four-, six-, and thirteen-story buildings.

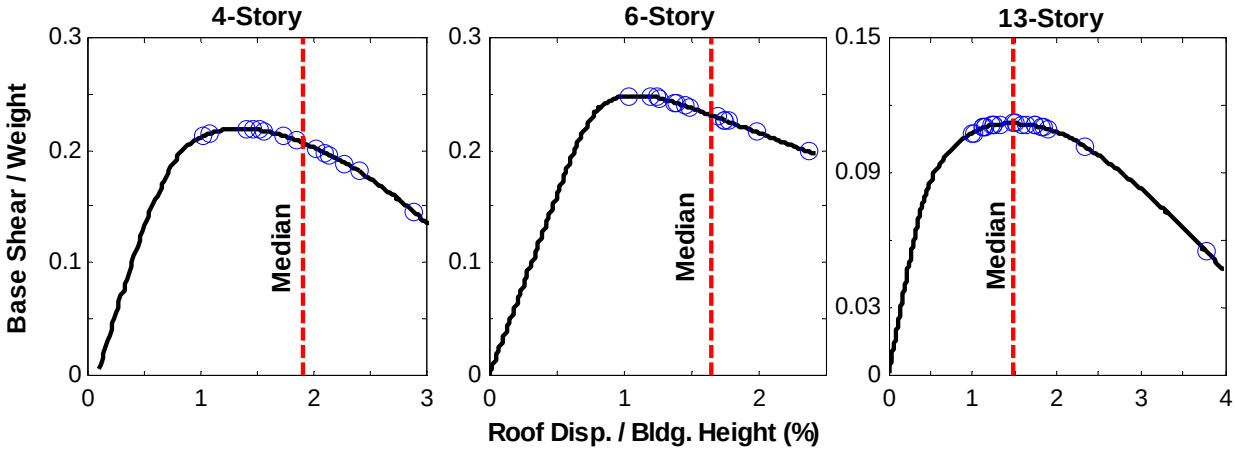

Figure 3: Roof displacements determined by nonlinear RHA of three buildings for 21 ground motions identified on first-mode pushover curves.

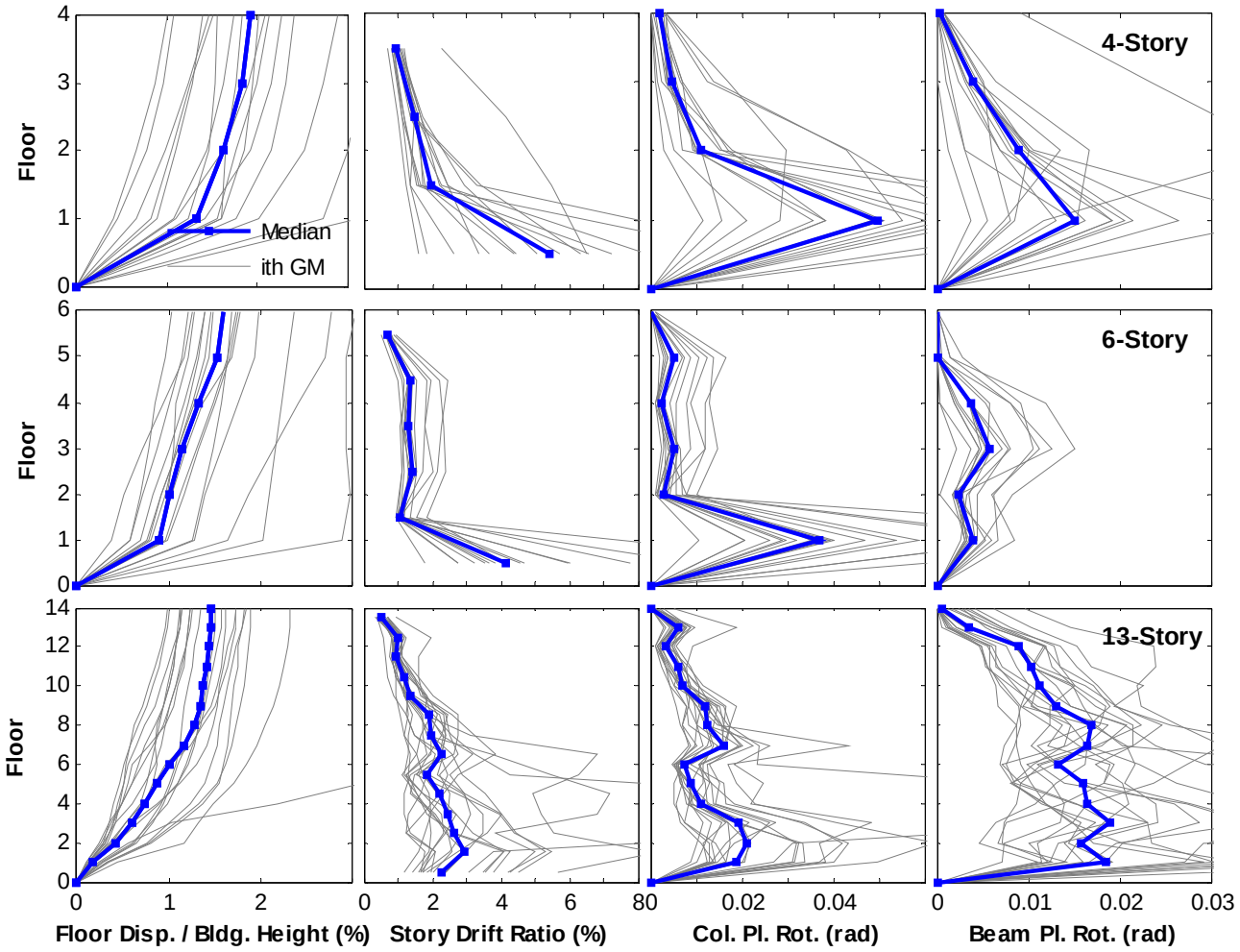

Figure 4: Median values of EDPs determined by nonlinear RHA of three buildings for 21 ground motions; results for individual ground motions are also included.

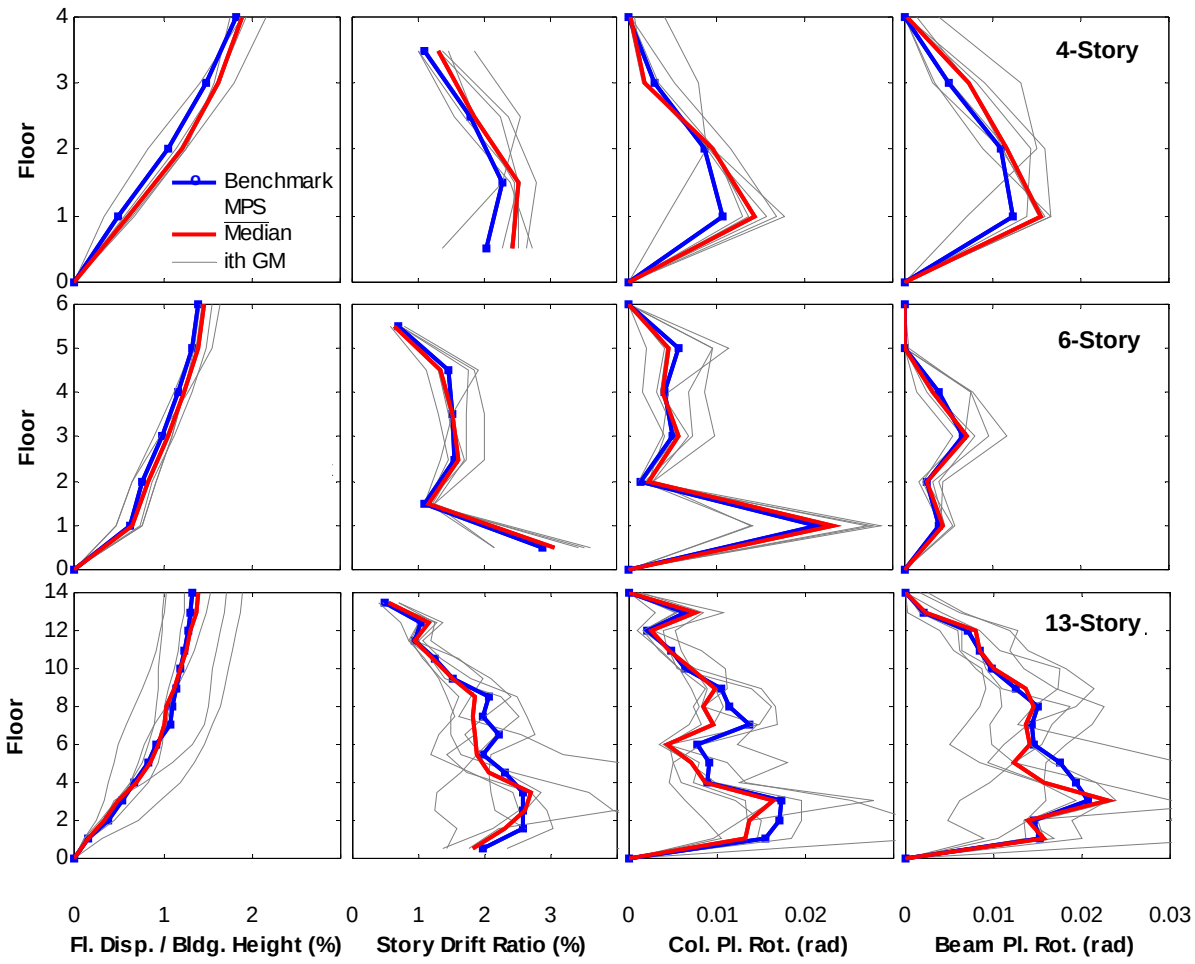

Figure 5: Comparison of median EDPs based on the MPS concept with benchmark EDPs for the 4-, 6-, and 13-story buildings for Ground Motion Set 1; individual results for each of the seven scaled ground motions are also presented.

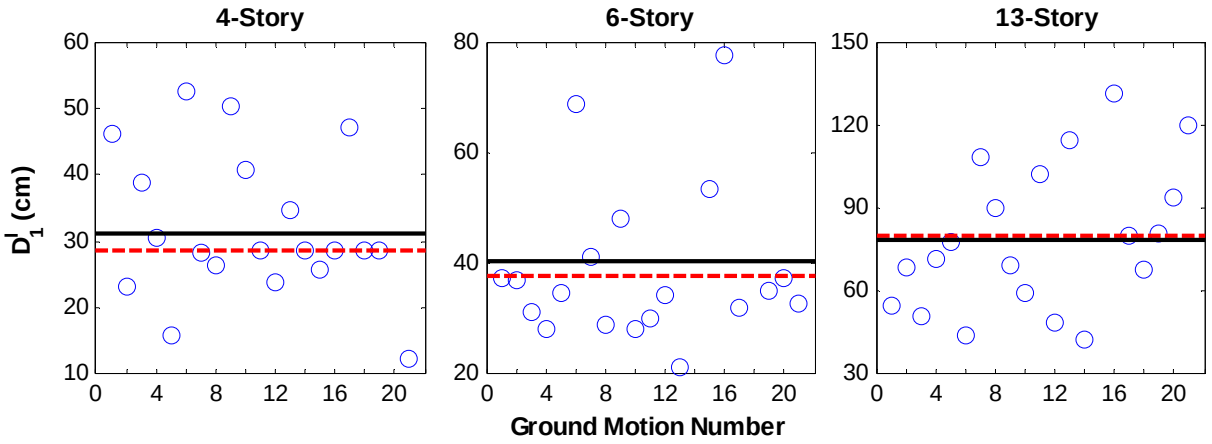

Figure 6: Peak deformation $\bar{D}_1^I$ values of the first-"mode" inelastic SDF system for 21 ground motions for 4-, 6-, and 13-story buildings; "exact" target value of deformation $\bar{D}_1^I$ is identified by horizontal continuous line; horizontal dashed line indicates target value of deformation $\bar{D}_1^I$ established by C_R equation.

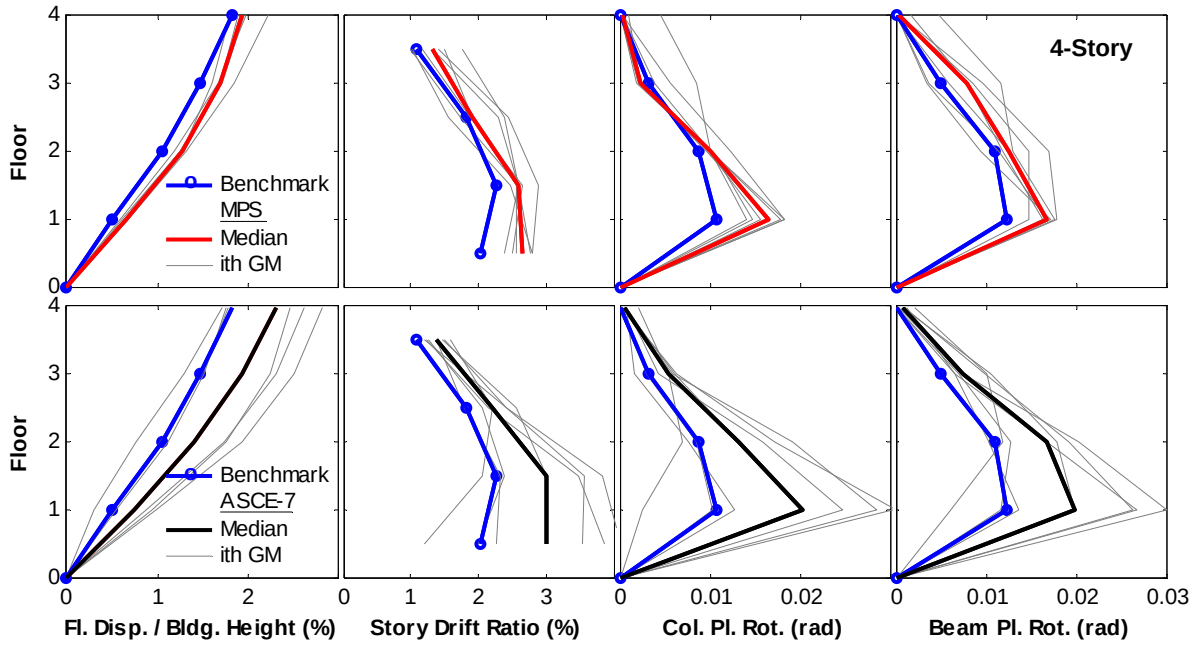

Figure 6: Comparison of median EDPs for Ground Motion Set 1 scaled according to MPS (top row) and ASCE-7 (bottom row) scaling procedures with benchmark EDPs; individual results for each of seven scaled ground motions are also presented. Results are for the 4-story building.

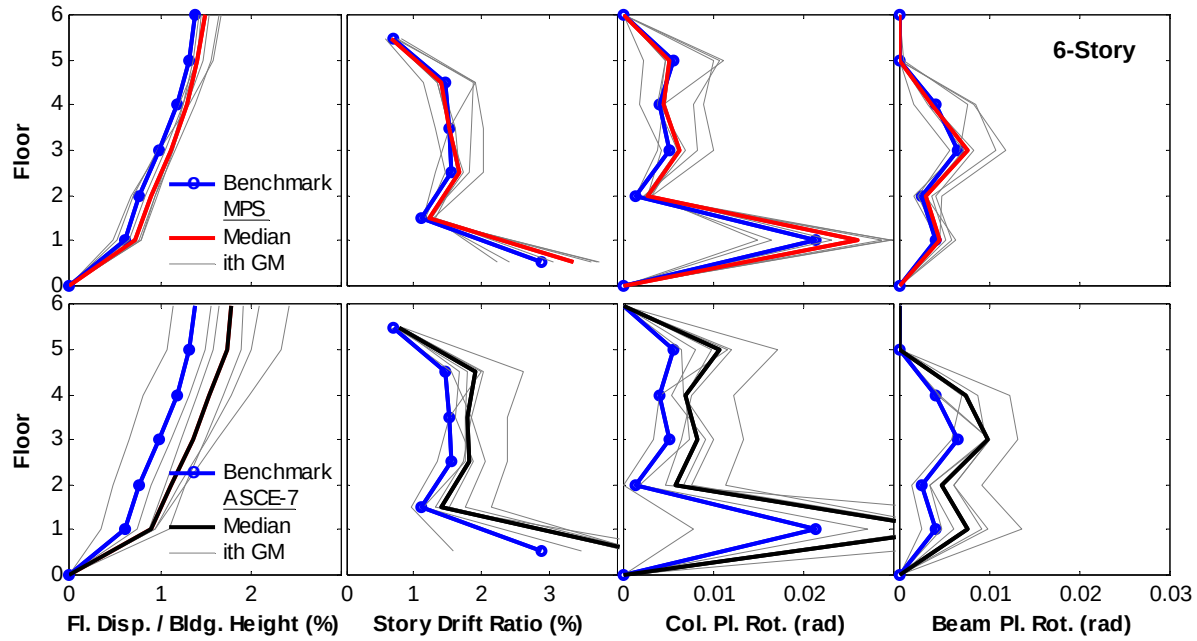

Figure 7: Comparison of median EDPs for Ground Motion Set 1 scaled according to MPS (top row) and ASCE-7 (bottom row) scaling procedures with benchmark EDPs; individual results for each of seven scaled ground motions are also presented. Results are for the 6-story building.

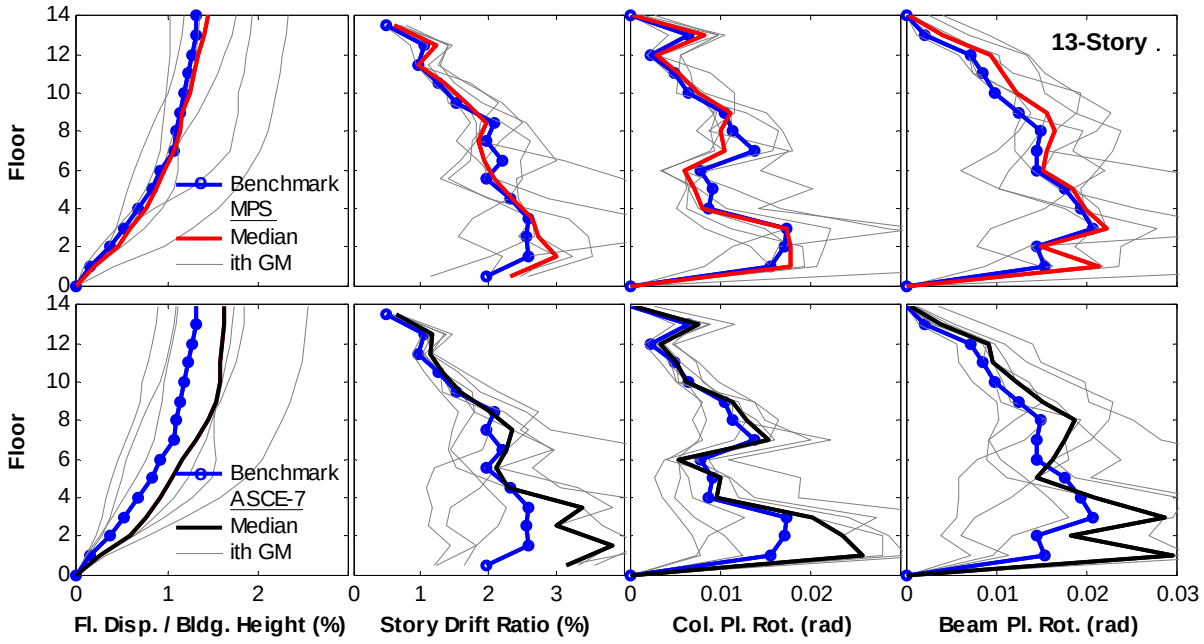

Figure 8: Comparison of median EDPs for Ground Motion Set 1 scaled according to MPS (top row) and ASCE-7 (bottom row) scaling procedures with benchmark EDPs; individual results for each of seven scaled ground motions are also presented. Results are for the 13-story building.

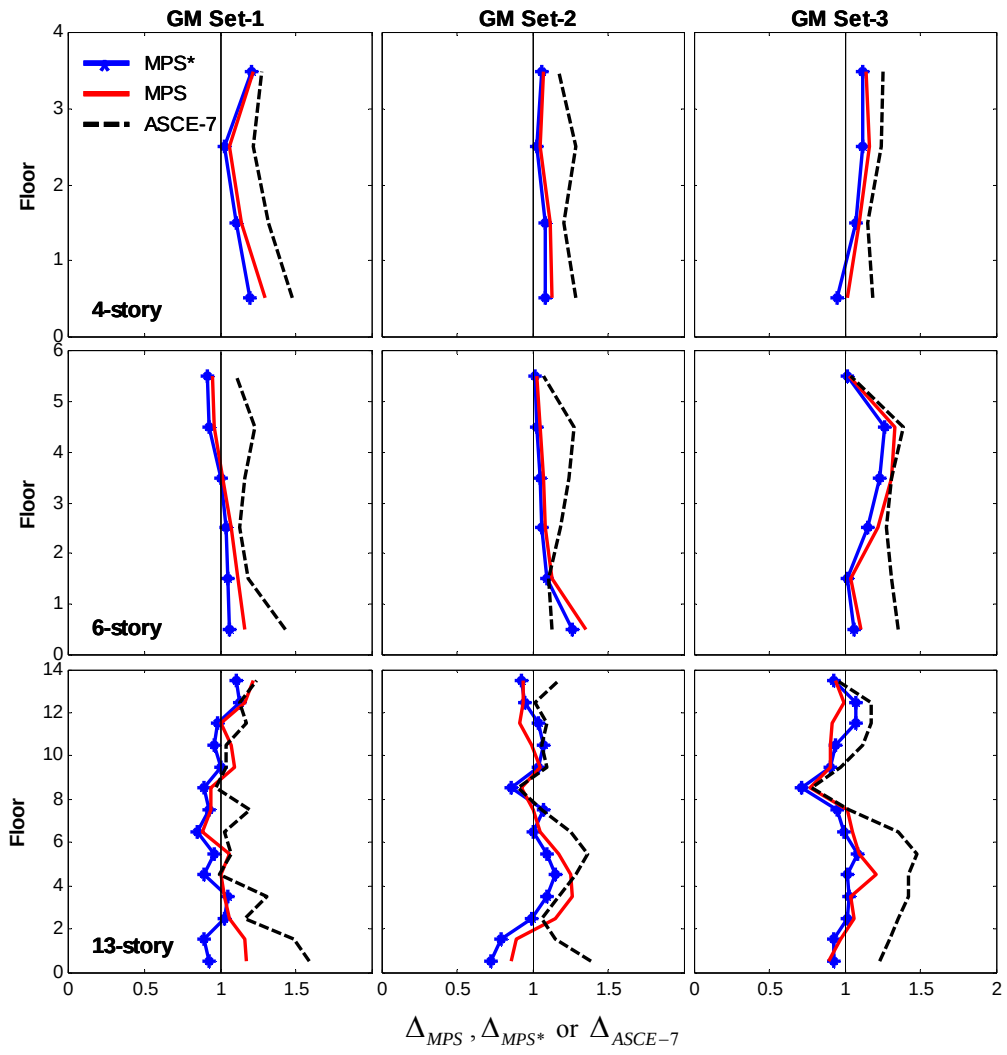

Figure 9: Median story drift ratios Δ_{MPS} , Δ_{MPS*} and Δ_{ASCE-7} for three ground motions sets and for three buildings.

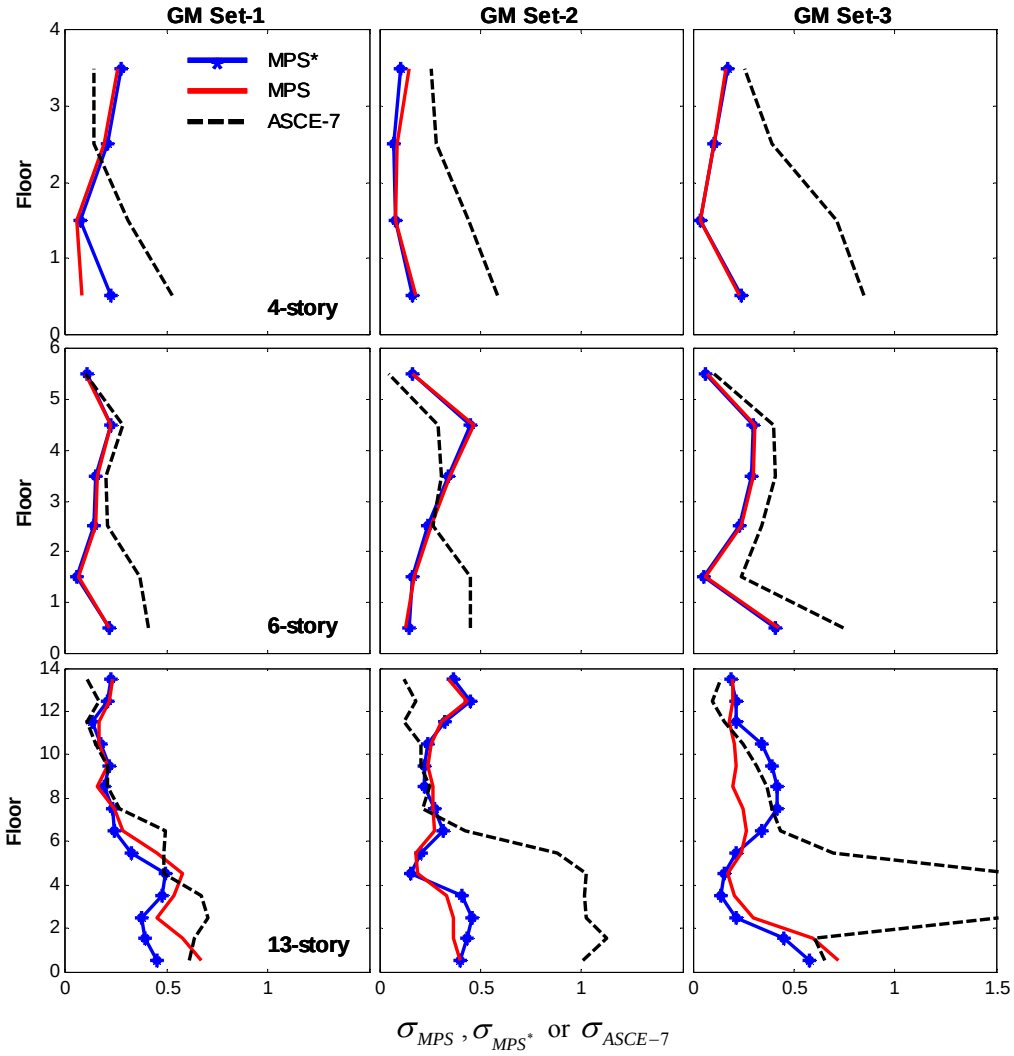

Figure 10: Dispersion of story drift ratios σ_{MPS} , σ_{MPS^*} and σ_{ASCE-7} for three ground motions sets and for three buildings.

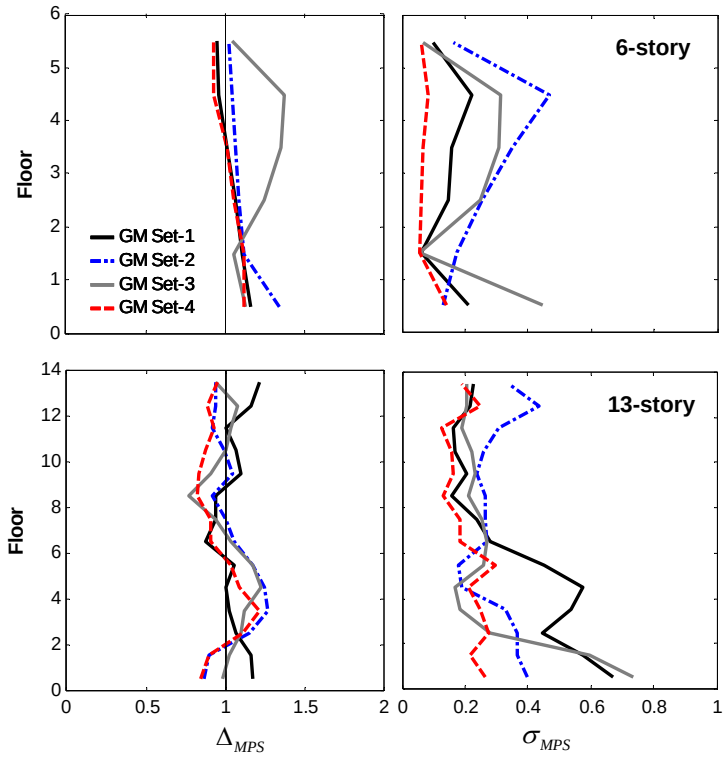

Figure 11: Median Δ_{MPS} and dispersion σ_{MPS} of story drift ratios for four ground motions sets and for two buildings.